A THEORETICAL STUDY OF MICROWAVE BEAM ABSORPTION BY A RECTENNA

James H. Ott
James S. Rice
Donald C. Thorn
Novar Electronics Corporation, Barberton, Ohio

ABSTRACT

The results of a theoretical study of microwave beam absorption by a Rectenna is given. Total absorption of the power beam is shown to be theoretically possible. Several improvements in the Rectenna design are indicated as a result of analytic modeling. The nature of Rectenna scattering and atmospheric effects are discussed.

INTRODUCTION

A workable Solar Power Satellite system will depend upon the efficient free-space transmission of energy to earth via an environmentally benign microwave beam. The "Rectenna", a large array of dipole-diode devices which captures and rectifies microwave power from satellites, embodies an emerging technology pioneered by William C. Brown[1] of Raytheon. Brown[2] and Richard Dickinson[3] of JPL have reported tests on experimental Rectenna arrays which have achieved microwave to dc conversion efficiencies exceeding 80%. However, classical antenna theory tells us that an isolated dipole must re-radiate as much energy as it delivers to a properly matched load. Because of a frequently expressed concern over whether or not this antenna theory was in contradiction with experimental Rectenna results, Novar Electronics Corporation undertook the task of developing a theoretical model which describes the absorption of a microwave beam by a very large Rectenna. In view of the size and scope of the SPS program, it is important to theoretically determine whether a rectenna array of the reference system design can totally absorb the power beam--that is, produce no scattering. In addition, it is desirable to study the microwave absorption process in order to provide a theoretical model for the simulation of design improvements and, because of concerns about possible electromagnetic interference from the rectenna, to obtain additional insights into the rectenna's scattering properties.

Novar's work demonstrates not only that the theoretical absorption limit is in fact 100% but that the number of elements required for total absorption per unit area can be greatly reduced, significantly reducing the cost of the Rectenna. Results further indicate that Rectenna panels can be made to totally absorb at any angle of incidence by adjusting reflector and element spacing and load impedance. This suggests a flat or terrain conforming Rectenna eliminating the need for the "billboard" or "Venetian blind" design and essentially conforming to the terrain. Also, the screen reflector should be able to be replaced by parasitic reflector dipole elements.

Deviations from conditions required for total absorption give rise to scattering, and the resulting losses due to variations from design center values for several parameters are shown. The directionality of fundamental and harmonic scattering from a Rectenna is described. Among the factors causing scattering that were studied are microwave beam depolarization amd amplitude fluctuations caused by disturbances in the atmosphere. Included in this category is "diffracted signal enhancement", the diffractive effects of large objects flying over the Rectenna, which can be expected to cause transient signal increases as large as 9 dB which must be taken into account in the rectenna design.

Because of the difficulty in trying to analyze a large array of interacting dipoles using mutual impedance analysis, it was necessary to develop another type of mathematical model descriptive of the microwave power absorption process. Two such models were derived from Maxwell's equations. These models quantify conditions for total absorption of the power beam by a Rectenna and provide values for scattering losses due to deviations in each condition.

CURRENT SHEET RECTENNA MODEL

The first model is based on the current sheet equivalency of a large planar array above a reflector as shown in Figure 1. The current sheet has the properties of resistive absorbers described by Jasik[4] and Kraus[5]. The model is mathematically characterized by an expression for the fraction of an incident plane wave's power that is reflected from the sheet.

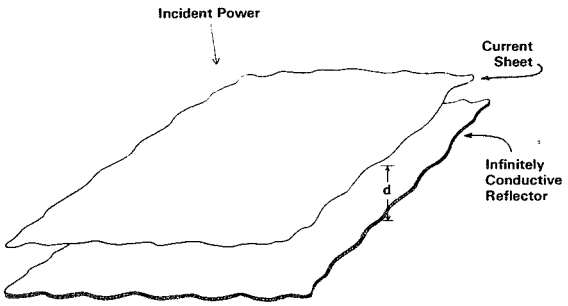

FIGURE 1
CURRENT SHEET RECTENNA MODEL

This expression, which agrees with Jasik, and for which no derivation could be found in the literature, is determined as follows. First, Maxwell's equations are solved to obtain general expressions for the electric and magnetic fields in the region above the current sheet and in the region between the current sheet and the reflector surface.

Next, the boundary conditions are satisfied at the infinitely conductive reflector surface and then at the current sheet as the thickness of the current sheet is allowed to become very thin. This yields expressions for the waves at the surface of the current sheet. The expressions are then solved simultaneously for the power reflection coefficient, the fraction of power reflected by the current sheet. It is expressed by either Equation 1a or 1b, following, depending upon the polarization of the incident wave.*

*Polarization is defined by the relationship of the incident wave's electric field vector, E, to the plane of incidence, the plane determined by rays in the directions of propagation of the incident and reflected waves. When E is parallel to the plane of incidence, the wave is said to be parallel polarized. When E is perpendicular to the plane, the wave is said to be perpendicularly polarized. (Any other polarization can be decomposed into a combination of parallel and perpendicular polarization.)

Parallel Polarization

$$|\rho_{\parallel}|^2 = \frac{\left(\frac{\sqrt{\mu/\varepsilon}}{R_o}\cos\theta - 1\right)^2 + \cot^2\left(\frac{2\pi d}{\lambda}\cos\theta\right)}{\left(\frac{\sqrt{\mu/\varepsilon}}{R_o}\cos\theta + 1\right)^2 + \cot^2\left(\frac{2\pi d}{\lambda}\cos\theta\right)} \quad (1a)$$

Perpendicular Polarization

$$|\rho_{\perp}|^2 = \frac{\left(\frac{\sqrt{\mu/\varepsilon}}{R_o}\sec\theta - 1\right)^2 + \cot^2\left(\frac{2\pi d}{\lambda}\cos\theta\right)}{\left(\frac{\sqrt{\mu/\varepsilon}}{R_o}\sec\theta + 1\right)^2 + \cot^2\left(\frac{2\pi d}{\lambda}\cos\theta\right)} \quad (1b)$$

where:

- R_o is the resistance of the current sheet in ohms per square* ,
- θ is the angle of incidence of the received wave as measured from the normal,
- d is the separation between the current sheet and reflector,
- λ is the wavelength,
- ε and μ are the permittivity and permeability, respectively.

The expressions above demonstrate that total absorption is theoretically possible for normal incidence ($\theta = 0$) when $d = \lambda/4$ and $R_o = \sqrt{\mu/\varepsilon} = 377$ ohms for free space. The power reflection coefficient and reflected power as functions of deviations in R_o, d, or θ from those values required for total absorption at normal incidence are shown in Figure 2.

The model further predicts that a Rectenna can be designed for total absorption for beam angles off normal incidence.† This leads to the possibility of a Rectenna that can be built to lie flat on the ground and be essentially "terrain conforming". This type of Rectenna array has several advantages over the "billboard" or "venetian blind" construction of the reference system: 1) much less excavation is required, 2) there is the potential to suspend the elements and reflector screen above farms, buildings, etc., and 3) less scattering is anticipated because there are no "billboard" edges to cause diffraction of the power beam.

This current sheet Rectenna model provides a "macroscopic view" of the microwave absorption process. Novar has developed a second model which provides an insight into the role played by the individual Rectenna elements. Moreover it provides an independent theoretical confirmation of the ability of the Rectenna to totally absorb the power beam.

WAVEGUIDE RECTENNA MODEL

The second model quantifies the electromagnetic modes (field configurations) in the immediate vicinity of a Rectenna element in the Rectenna array and gives limits for the element spacing which permit total power beam absorption by preventing unwanted modes from propagating (scattering). This model is based on the properties of a special waveguide described by Wheeler[6] in his analysis of certain aspects of a large planar array. Specifically, the waveguide has special "imaging" characteristics and has the ability to allow only plane wave propagation. The waveguide is rectangular in shape with a probe (monopole) inserted through the middle of one of the walls. However unlike "conventional" waveguides, the two walls parallel to the monopole are nonconductive and "magnetic" ($\mu = \infty$, $\sigma = 0$), with the other two walls being perfectly conductive ($\sigma = \infty$). When we solve the equations describing the nature of wave reflections at

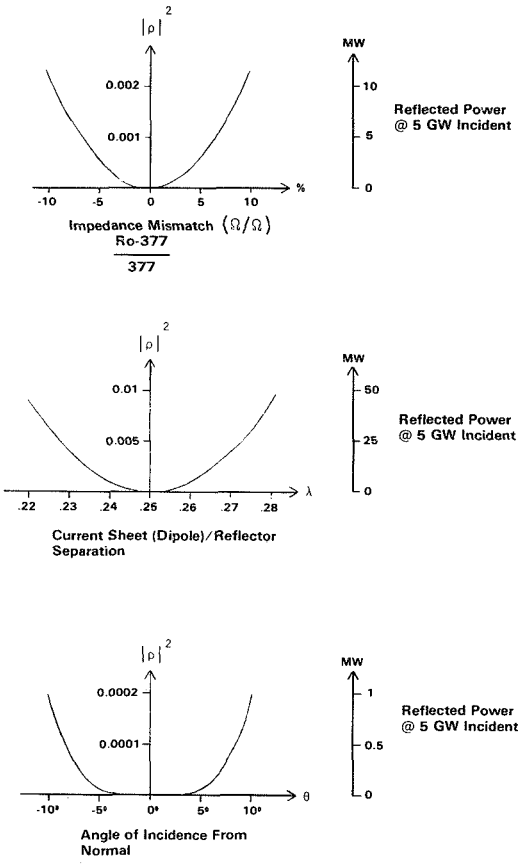

FIGURE 2
POWER REFLECTION COEFFICIENT AND REFLECTED POWER LEVEL OF THE CURRENT SHEET RECTENNA MODEL AS A FUNCTION OF VARIOUS PARAMETERS

*Resistance per square is the resistance between opposite edges of a square slab of resistive material and therefore is independent of the size of the square.

†With λ fixed, and given any θ, there is an R_o and d such that $|\rho|^2 = 0$.

the walls, it is found that a monopole in this type of waveguide, which we will call a "mixed-wall" waveguide, produces an infinite array of image dipoles with currents of identical magnitude and phase as depicted in Figure 3.* Conversely, an infinite array of identical dipoles with currents of identical magnitude and phase can be replaced by a single monopole in a mixed-wall waveguide to analyze the behavior of a dipole as illustrated by Figure 4. Since the power beam is nearly uniform in power density over quite a large area, dipoles within a fairly large arbitrarily selected area of the Rectenna will have currents nearly uniform in magnitude and phase which can be closely approximated for that area by an infinite array. Thus the behavior of a dipole which defines the center of this area can be accurately modeled by the behavior of a monopole in a mixed-wall waveguide.

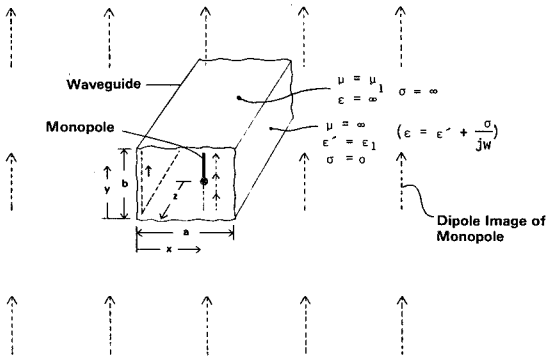

FIGURE 3
IMAGING PROPERTIES OF MIXED-WALL WAVEGUIDE WITH MONOPOLE

The first step in analysis of this monopole's behavior is to determine what modes can propagate in the mixed-wall waveguide† and under what conditions. We want the TEM mode to be the only mode that can propagate. This TEM mode is the same field configuration as that of the power beam, i,e., a plane wave. If other modes propagate, scattering is taking place. Since the side walls of a mixed-wall waveguide as shown in Figure 3 are non-conductive and "magnetic", the mixed-wall waveguide is similar to a strip-line for the TEM modes. Thus this waveguide will support the TEM mode at the power beam frequency independent of the waveguide dimensions.

Next, the properties of the mixed-wall waveguide for the higher order modes are derived in order not only to determine the conditions required for their evanescence but also to allow us to describe the near fields around the monopole. To do this, Maxwell's equations are solved to obtain wave equations which are then modified by mathematical decomposition to put them into an efficient form for solution. The wave equations are then solved to obtain general equations for the magnetic and electric fields in the mixed-wall waveguide. These equations are functions of pairs of integers, one integer of which is associated with the "a" dimension in Figures 3 and 4, and the other with "b". Specific values for the integers in a pair defines a mode. The higher order modes have either transverse magnetic or transverse electric fields.‡ These are respectively designated the TM_{fg} and the TE_{mn} modes, where f and n are 0,1,2,3,...; g and m are 1,2,3,....

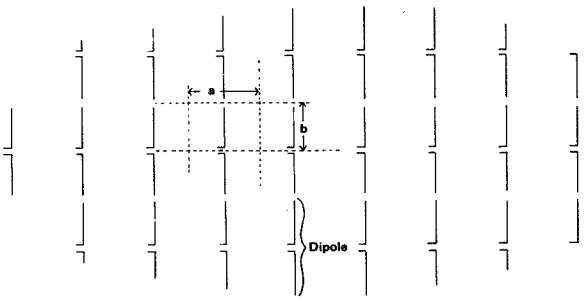

FIGURE 4
SECTION OF INFINITE ARRAY OF DIPOLES MODELED BY A MONOPOLE IN A "MIXED-WALL" WAVEGUIDE

Inspection of the mode equations shows that the lowest cutoff frequency for higher order TM modes is associated with TM_{01} and that for the TE modes is the TE_{10}. This means that at a given frequency the smallest critical dimensions for propagation are associated with those two modes. The next larger critical dimension is associated with the TE_{20}.

The TE_{10} mode is actually non-existent in our mixed-wall waveguide/monopole configuration because it is not generated when the monopole is located in the center of this special type of waveguide.** This results in the critical dimensions for higher mode

*Analogous to the study of optical reflections from mirrors, the "method of images" shows that the fields within the mixed-wall waveguide boundaries are the same as though there was no waveguide but only the monopole and an infinite number of identical magnitude and phase images.

†Modes, which are the various field configurations that can exist within a waveguide, have the property that for a given frequency they are evanescent (non-propagating) for waveguide dimensions less than certain critical values, which are called "cutoff" dimensions, and can propagate for any dimensions greater than those values. Each mode has its own set of cutoff dimensions. Conversely, for a given set of waveguide dimensions, there is a critical frequency for each mode (called the cutoff frequency) below which the mode is evanescant and above which it can propagate.

‡Transverse means no component in the $\pm$ z direction in Figure 3.

**Note that "mode-hopping", the generation of modes due to waveguide imperfections, is not a problem here because the waveguide is assumed to be ideal.

propagation being determined by the TM_{01} and the TE_{20}. Specifically, for evanescence of all higher modes, those critical dimensions restrict the waveguide dimensions to be less than one wavelength in the "a" direction and less than one half wavelength in the "b" direction. (This is equivalent to a Rectenna element spacing of just under one wavelength.)

The total electric field, $\underline{E}$, and the total magnetic field, $\underline{H}$, in the mixed-wall waveguide are each sums of the various field configurations or modes that exist in the waveguide. Now $\underline{E}$ and $\underline{H}$ are vector sums of respective field components in the x, y, and z directions of Figure 3. Thus for " + z directed" field components, $\underline{E}$ and $\underline{H}$ can be represented by the equations given in Table I, where A_{mn} and B_{fg} are respectively the maximum amplitudes of H_z and E_z, K_{oo} is the maximum amplitude of the $\underline{H}$ field of the TEM wave. The α's and β's at the bottom of the table are respectively the real and imaginary parts of the expressions shown for the γ's. The terms involving double summations represent the "sums of the higher order modes". The leading terms in the equations for E_y and H_x are the equations for the TEM mode. If the higher order modes are evanescent, then the double summation terms are components of the fields associated with reactive power.

If a reflector or shorting plate is inserted in the waveguide behind the monopole, as shown in Figure 5, the situation is equivalent to the infinite array of dipoles in Figure 4 being backed by a reflector. A set of equations analagous to those in Table I can then be generated for the "-z directed" field components of the waves reflected from the shorting plate. Summing the +z and -z directed field components in the neighborhood of the monopole gives rise to a set of equations of the same form as those in a conventional waveguide backed by a shorting plate. These equations establish matching requirements on the monopole and load impedances and spacing of the monopole from the shorting plate so that the non-evanescent wave does not propagate back up the waveguide toward the source. Since it is well known that a probe in a conventional waveguide backed by a shorting plate can totally absorb all power flowing down the waveguide[7], it is therefore expected that a probe (monopole) in a mixed-wall waveguide can also totally absorb all power flowing down that type of waveguide. Therefore total absorption of the plane wave power beam by a dipole in a Rectenna is expected when the separation between dipoles is within limits dictated by the mixed-wall waveguide model's dimensions which restrict propagation in that waveguide to the TEM mode.

Since the waveguide dimensions which restrict propagation to the TEM mode is less than λ in the "a" direction and less than $\lambda/2$ in the "b" direction of Figures 3 and 4, and since the separation between the centers of the dipoles is "a" by "2b" as can be seen from Figure 4, then the maximum allowable separation of the centers of dipoles for total absorption of a plane wave, for the rectangular grid configuration of Figure 4, is just under one wavelength.

$$H_z = 0 + \sum_{m=1}^{\infty}\sum_{m=0}^{\infty} A_{mn} \sin\frac{m\pi x}{a} \cos\frac{m\pi y}{b} e^{-\alpha_{mn} z}$$

$$E_z = 0 + \sum_{f=0}^{\infty}\sum_{g=1}^{\infty} B_{fg} \cos\frac{f\pi x}{a} \sin\frac{g\pi y}{b} e^{-\alpha_{fg} z}$$

$$E_x = 0 + \sum_{m=1}^{\infty}\sum_{n=0}^{\infty} \frac{j\omega\mu n\pi}{k_{cmn}^2 b} A_{mn} \sin\frac{m\pi x}{a} \sin\frac{m\pi y}{b} e^{-\alpha_{mn} z}$$

$$+ \sum_{f=0}^{\infty}\sum_{g=1}^{\infty} \frac{-\alpha_{fg} f}{k_{cfg}^2 a} B_{fg} \sin\frac{f\pi x}{a} \sin\frac{g\pi y}{b} e^{-\alpha_{fg} z}$$

$$E_y = \frac{\mu}{\epsilon} K_{oo} e^{-j\beta_{oo} z} + \sum_{m=1}^{\infty}\sum_{n=0}^{\infty} \frac{j\omega\mu m\pi}{k_{cmn}^2 a} A_{mn} \cos\frac{m\pi x}{a} \cos\frac{m\pi y}{b} e^{-\alpha_{mn} z}$$

$$+ \sum_{f=0}^{\infty}\sum_{g=1}^{\infty} \frac{\alpha_{fg} g\pi}{k_{cfg}^2 b} B_{fg} \cos\frac{f\pi x}{a} \cos\frac{a\pi y}{b} e^{-\alpha_{fg} z}$$

$$H_x = K_{oo} e^{-j\beta_{oo} z} + \sum_{m=1}^{\infty}\sum_{n=0}^{\infty} \frac{\alpha_{mn} m\pi}{k_{cmn}^2 a} A_{mn} \cos\frac{m\pi x}{a} \cos\frac{m\pi y}{b} e^{-\alpha_{mn} z}$$

$$+ \sum_{f=0}^{\infty}\sum_{g=1}^{\infty} \frac{j\omega\varepsilon g\pi}{k_{cfg}^2 b} B_{fg} \cos\frac{f\pi x}{a} \cos\frac{g\pi y}{b} e^{-\alpha_{mn} z}$$

$$H_y = 0 + \sum_{m=1}^{\infty}\sum_{n=0}^{\infty} \frac{-\alpha_{mn} n\pi}{k_{cmn}^2 b} A_{mn} \sin\frac{m\pi x}{a} \sin\frac{m\pi y}{b} e^{-\alpha_{mn} z}$$

$$+ \sum_{f=0}^{\infty}\sum_{g=1}^{\infty} \frac{j\omega\varepsilon g\pi}{k_{cfg}^2 b} B_{fg} \sin\frac{f\pi x}{a} \sin\frac{g\pi y}{b} e^{-\alpha_{fg} z}$$

$$\gamma_{mn} = \alpha_{mn} + j\beta_{mn} = \sqrt{k^2 - \left(\frac{m\pi}{a}\right)^2 - \left(\frac{n\pi}{b}\right)^2} = \sqrt{k^2 - k_{cmn}^2}$$

$$\gamma_{fg} = \alpha_{fg} + j\beta_{fg} = \sqrt{k^2 - \left(\frac{f\pi}{a}\right)^2 - \left(\frac{g\pi}{b}\right)^2} = \sqrt{k^2 - k_{cfg}^2}$$

$$\beta_{oo} = k = \frac{2\pi}{\lambda}$$

TABLE I

ELECTROMAGNETIC FIELD EQUATIONS FOR A MIXED-WALL WAVEGUIDE

Equations shown are for total " + z directed" portion of the field components in a mixed-wall waveguide. With appropriate sign changes, equations express the " – z directed" components.

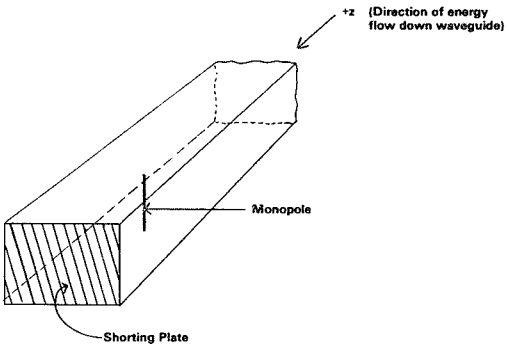

FIGURE 5
MONOPOLE IN MIXED-WALL WAVEGUIDE BACKED BY SHORTING PLATE

ELEMENT DENSITY

The existence of non-evanescent higher order modes corresponds to the existence of grating lobes. Analysis of the generation of grating lobes indicates that the maximum separation between dipole centers for avoidance of grating lobes with the triangular grid configuration used in the Reference System is just under 1.15λ. It is understood that the present separation between dipole centers in the Reference System is just unver 0.6λ. The number of Rectenna dipole-diode elements needed for total power beam absorption can be significantly reduced over the number needed for the Reference Systems as shown below.

	NUMBER OF DIPOLE-DIODE ELEMENTS REQUIRED (NORMAL INCIDENCE)
Reference System Design	18 billion
Triangular Grid Configuration With Maximum Allowable Dipole Spacing	4.5 billion
Rectangular Grid Configuration With Maximum Allowable Dipole Spacing	5.2 billion

In additon, greater diode efficiency is indicated when the number of Rectenna dipole elements is reduced since the power density per diode is higher.

PARASITIC REFLECTING DIPOLES

Total absorption of energy by the monopole in a conventional waveguide requires that the shorting plate in the waveguide by approximately a quarter wavelength behind the monopole. This distance is also expected to be proper for the mixed-wall waveguide. Since the shorting plate corresponds to the Rectenna reflector, and since it is expected that the shorting plate can be replaced by a parasitic reflecting monopole as can be done easily in a conventional waveguide and still totally absorb the energy traveling down the waveguide, then the Rectenna reflector should be replaceable by parasitic dipole elements, as depicted in Figure 6.

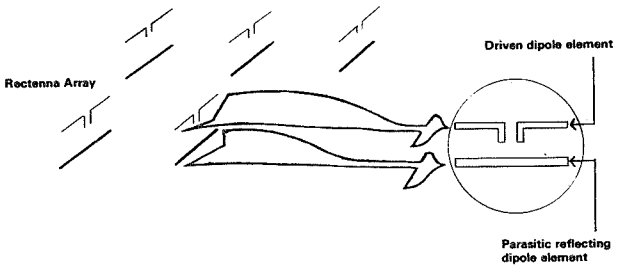

FIGURE 6
RECTENNA WITH PARASITIC REFLECTING DIPOLE ELEMENTS

HARMONIC FILTER

None of the preceeding analysis permits the dipole terminals to see a non-linear load for total absorption. What is required in a Rectenna element for total absorption is a harmonic filter, as depicted in Figure 7, that presents a linear load to the dipole terminals at the fundamental frequency such that the load voltage and current seen by the dipole are pure sinusoids not in phase quadrature, i.e. that the linear load has a real component.

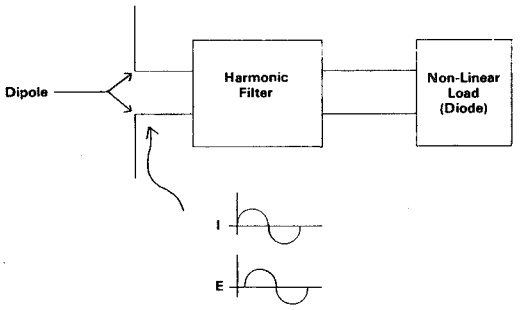

FIGURE 7
RECTENNA ELEMENT HARMONIC FILTER

FUNDAMENTAL SCATTERING

Specular scattering of the power beam, depicted in Figure 8, is expected to result from most deviations in the Rectenna's parameters. The smaller the deviation anomaly, the broader will be the specular lobe. Single, isolated element failures (short or open diodes) will appear to radiate as isotropic sources above a reflector.

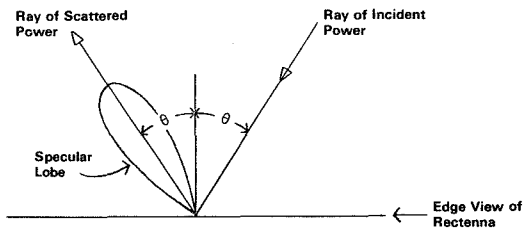

FIGURE 8
DEPICTION OF SPECULAR SCATTERING FROM FACE OF RECTENNA
-Frequency is the power beam fundamental

HARMONIC SCATTERING

The Rectenna dipole-filter-diode assembly and power bus are expected to be most significant sources of harmonic scattering. The harmonic energy will be concentrated in grating lobes, as shown in Figure 9. Random Rectenna imperfections will broaden the lobes.

ATMOSPHERIC EFFECTS

Atmospheric phenomena cause polarization shifts and amplitude fluctuations in an electromagnetic wave at microwave frequencies [8,9,10,11,12,13]. However, only infrequent depolarizing events up to 20 dB (1% scattered power) have been observed in microwave downlink transmissions with greater than 10 meter apertures. Based on these observations, depolarization is not expected to be a significant source of scatter.

Amplitude fluctuations cause scattering by disrupting the uniform illumination of the Rectenna. In addition, this disruption of the RF power level from design values for the diodes causes impedance mismatches resulting in further scattering. Existing earth-space propagation measurements to date [13] indicate a maximum of 0.1 dB amplitude fluctuations for 2-3 GHz at elevation angles above 20° (which would cause insignificant scattering).

There are factors which impair the application of previous earth station measurements to the SPS. In all studies found, there is significant aperture averaging. The minimum aperture area for those studies is about $5000\lambda^2$ as compared to about $1\lambda^2$ or so of each "independent" receiving element in the Rectenna. This indicates that the amplitude fluctuations may be appreciably greater than 0.1 dB for the Rectenna. Another factor is that the measurement data, taken at C and S bands, were obtained from modulated signals. Most deep fades are frequency sensitive. Therefore for modulated signals, which have their power spread over a spectrum of frequencies, the observed amplitude fluctuations would be expected to be less than those of the monochromatic SPS power beam.

As of this writing, Novar Electronics Corporation intends to receive, at its earth station located in Summit County, Ohio, special monochromatic calibration signals from RCA's new F3 Satcom* in order to observe aperture averaging effects and monochromatic signal fading characteristics. Aperture areas of approximately $1200\lambda^2$ and on the order of $1\lambda^2$ will be used to comparatively receive the signals (which are transmitted for satellite installation test purposes to determine EIRP countours).

*Scheduled to be stationed in orbit at the end of December, 1979

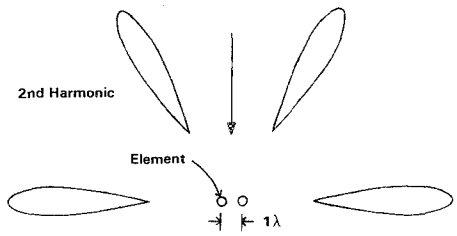

FIGURE 9a
EXAMPLE OF ELEVATION OF HARMONIC RADIATION

Figure depicts 2nd harmonic scattering for normal incidence of power beam when the element spacing is equal to λ at the fundamental frequency.

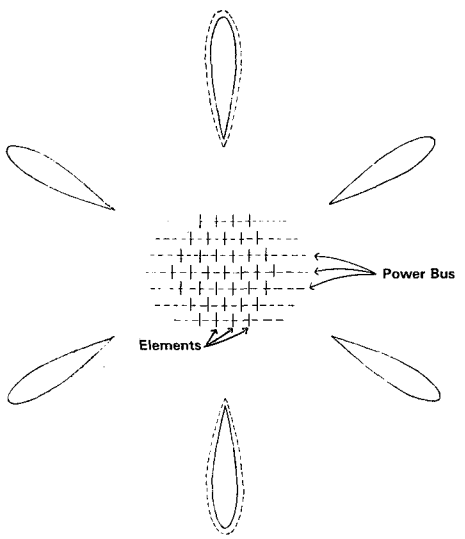

FIGURE 9b
AZIMUTHS OF HARMONIC RADIATION

"Dotted" lobe due to power bus.

FIGURE 9
GRATING LOBE NATURE OF HARMONIC SCATTERING FROM A RECTENNA

DIFFRACTED SIGNAL ENHANCEMENT

A large object flying through the power beam over the Rectenna causes diffraction patterns to be generated at the Rectenna as depicted in Figure 10. Preliminary experimental evidence has been obtained. Depending on the size and shape of the object, increases in signal levels as large as 9 dB are possible. Therefore, Rectenna diodes should have tolerance to the resulting spot-transient signal enhancement to protect against overvoltage transients from fast aircraft and also against diode overheating from slower objects.

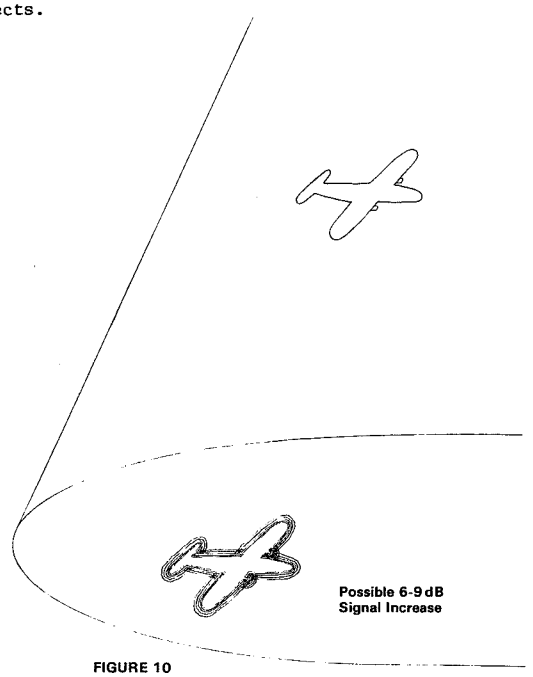

FIGURE 10
DIFFRACTION ENHANCEMENT AT RECTENNA CAUSED BY OBJECT FLYING THROUGH THE POWER BEAM

CONCLUSIONS

Analytic modeling shows that it is theoretically possible for a Rectenna to totally absorb microwave energy, i.e., produce no scattering. The number of elements required is significantly less than indicated in the Reference System. The Rectenna can be designed for total absorption at off-normal angles of incidence and it is expected that the Rectenna's reflecting screen can be replaced with parasitic reflecting dipoles.

Further space-earth transmission studies are required. The application of existing data to the SPS is impaired because these were from measurements of modulated signals received by large aperture antennas.

REFERENCES

1. W. C. Brown, "The Technology and Application of Free-Space Power Transmission by Microwave Beam," Proceedings of the IEEE, Vol. 62, No. 1, January 1974, pp. 11-25.

2. W. C. Brown: "Optimization of the Efficiency and Other Properties of the Rectenna Element," 1976 IEEE MTT-S International Microwave Symposium Digest of Technical Papers, pp. 142-144.

3. R. M. Dickinson: "Performance of a High-Power 2.388-GHz Receiving Array in Wireless Power Transmission Over 1.54 km", 1976 IEEE MTT-S International Microwave Symposium Digest of Technical Papers, pp. 139-141.

4. H. Jasik (Ed): Antenna Engineering Handbook, McGraw-Hill Book Company, 1961. (The Salisbury screen is described in Sec. 32, page 36.)

5. J. D. Kraus: Electromagnetics, McGraw-Hill Book Company, Inc., 1953. (The "Space cloth" is discussed, starting on page 407.)

6. H. A. Wheeler: "The Radiation Resistance of an Antenna in an Infinite Array or Waveguide" Proc. I.R.E. Vol. 36, No. 4, April 1948, pp. 478-487. (Introduces concept of waveguide to image interchange) (Gives radiation resistance of each element of an infinite rectangular arry on the basis of a special waveguide.) (States ability of individual antenna in guide with reflector to have 100% absorption.)

7. J. C. Slater: Microwave Transmission. McGraw Hill Book Company, Inc., 1942 (Good basic treatment including a careful discussion of the limitation of "impedance" in waveguides. Discusses dipole-waveguide connection on page 296.)

8. R. R. Taur: "Ionospheric Scintillation at Frequencies Above 1 GHz" Comsat Technical Review, Vol. 4, No. 2. Fall, 1974.

9. J. P. Basart, G. K. Miley, and B. G. Clark: "Phase Measurements with an Interferometer Baseline of 11.3 km" IEEE Trans. on Antennas and Propagation. Vol. AP18, No. 3, May 1970, pp. 375-379. (Provides a good insight into phase variations due to the atmosphere.)

10. D. J. Fang: "Attenuation and Phase Shift of Microwaves due to Canted Raindrops" Cosmat Technical Review Vol. 5, No. 1. Spring, 1975.

11. D. J. Fang and J. Jih: "A Model of Microwave Propagation Along an Earth Satellite Path" Cosmat Technical Review Vol. 6, No. 2. February 1976.

12. M. C. Thompson, Jr. and H. B. James: "Antenna Aperature Size Effect on Tropospheric Phase Noise" IEEE Transactions on Antennas and Propagation Vol. AP. November, 1966. pp. 800-802.

13. R. K. Crane and D. W. Blood: "Handbook for the Estimation of Microwave Propagation Effects--Link Calculations for Earth-Space Paths (Path Loss and Noise Estimation)" Environmental Research & Technology, Inc. Technical Report No. 1, p. 7376 - TR1, June 1979.

In addition to the publications listed above, the authors gratefully acknowledge the assistance provided in personal communications from R. K. Crane, D. J. Fang, P. W. Hannan, R. K. Moore, R. R. Taur, and H. A. Wheeler.